JOURNAL OF MOLECULAR SPECTROSCOPY **131**, 261–271 (1988)

The Discovery of Two New Infrared Electronic Transitions of C_2: $B^1\Delta_g$–$A^1\Pi_u$ and $B'\,^1\Sigma_g^+$–$A^1\Pi_u$

M. DOUAY,[1] R. NIETMANN, AND P. F. BERNATH[2]

Department of Chemistry, University of Arizona, Tucson, Arizona 85721

Two new infrared electronic transitions of C_2, $B^1\Delta_g$–$A^1\Pi_u$ and $B'\,^1\Sigma_g^+$–$A^1\Pi_u$, were observed by Fourier transform emission spectroscopy of hydrocarbon discharges. A set of spectroscopic constants were derived for each vibrational level and then reduced to equilibrium constants, including

	T_e (cm^{-1})	ω_e (cm^{-1})	r_e (Å)
$B^1\Delta_g$	12 082.3360(40)	1407.4653(13)	1.38548
$B'\,^1\Sigma_g^+$	15 409.1390(39)	1424.1189	1.37735

RKR curves and Franck–Condon factors were calculated from the equilibrium constants.

I. INTRODUCTION

During the course of our spectroscopic observation of the $d^1\Sigma^+$–$b^1\Pi$ transition of SiC (*1*), A. D. McLean pointed out that the corresponding C_2 transition ($B'\,^1\Sigma_g^+$–$A^1\Pi_u$) had not been reported. This was quite surprising because the C_2 molecule occurs in such a wide variety of sources and has been studied for many years (see the preceding paper (*2*) for references). Examination of two previously recorded spectra disclosed the $B'\,^1\Sigma_g^+$–$A^1\Pi_u$ and $B^1\Delta_g$–$A^1\Pi_u$ transitions, in addition to the well-known Phillips system, $A^1\Pi_u$–$X^1\Sigma_g^+$, and Ballik–Ramsay system, $b^3\Sigma_g^-$–$a^3\Pi_u$. Our reanalysis of the Phillips System is reported in the preceding paper (*2*).

The $B^1\Delta_g$ and $B'\,^1\Sigma_g^+$ states of C_2 are predicted to be low-lying bound states by ab initio calculation (*3–6*). These two states do not connect with the ground $X^1\Sigma_g^+$ state via one-photon electric dipole selection rules. The infrared electronic transitions $B^1\Delta_g$–$A^1\Pi_u$ and $B'\,^1\Sigma_g^+$–$A^1\Pi_u$, however, are quite strong (Figs. 1–4). The main difficulty is that the Ballik–Ramsay and Phillips systems (as well as the usual collection of impurities such as CO, CN, CH, and ArH) make the infrared emission spectra of hydrocarbon discharges quite complex.

[1] Present address: Lab. de Spectroscopie des Molécules Diatomiques, CNRS UA779, Université des Sciences et Techniques de Lille, Bât. P5, 59655 Villeneuve d'Ascq Cedex, France.

[2] Alfred P. Sloan Fellow; Camille and Henry Dreyfus Teacher–Scholar.

0022-2852/88 $3.00

TABLE I

The Observed Line Positions of the $B^1\Delta_g$–$A^1\Pi_u$ Transition of C_2 (in cm^{-1})

A. 0-0 BAND

J	R_{ff}	O-C	Q_{ef}	O-C	P_{ff}	O-C
2.0	3598.5235	18	3589.7901	-5		
4.0	3602.1997	8	3587.6499	-6	3576.0043	-44
6.0	3604.6484	-12	3584.2845	0	-	-
8.0	3605.8703	-25	3579.6966	2	3556.4245	-4
10.0	3605.8703	26	3573.8854	0	3544.8056	4
12.0	3604.6329	-3	3566.8510	-7	3531.9682	-6
14.0	3602.1683	-4	3558.5931	-28	3517.9179	1
16.0	3598.4748	13	3549.1185	0	3502.6504	-30
18.0	3593.5506	37	3538.4201	0	3486.1780	1
20.0	3587.3877	-7	3526.5009	-3	3468.4925	-2
22.0	3579.9982	6	3513.3631	1	-	-
24.0	3571.3738	-2	3499.0064	6	-	-
26.0	3561.5179	3	3483.4302	-6	3408.2018	4
28.0	3550.4273	-4	-	-	3385.7000	8
30.0	3538.1057	11	3448.6306	-8	3361.9979	-3
32.0	-	-	3429.4084	-8	3337.1040	31
34.0	3509.7581	2	3408.9743	6		
36.0			3387.3217	-41		
38.0			3364.4671	-3		

J	R_{ee}	O-C	Q_{fe}	O-C	P_{ee}	O-C
1.0	3596.2240	2				
3.0	3600.5193	34	3588.8743	-9		
5.0	3603.5870	35	3586.1264	7	3571.5757	-4
7.0	3605.4280	23	3582.1547	4	3561.7937	45
9.0	3606.0425	10	3576.9617	4	3550.7806	-42
11.0	3605.4280	-19	3570.5471	0	3538.5636	-11
13.0	3603.5870	-32	3562.9123	3	3525.1302	-3
15.0	3600.5193	-23	3554.0566	0	3510.4836	-1
17.0	3596.2240	4	3543.9812	0	3494.6262	-1
19.0	3590.6971	18	3532.6867	-1	3477.5607	7
21.0	3583.9358	-6	3520.1733	-5	3459.2860	-7
23.0	3575.9458	-6	3506.4426	-5	3439.8081	-3
25.0	-	-	3491.4944	-11	3419.1241	-31
27.0	3556.2726	7	3475.3344	23	3397.2464	10
29.0	3544.5889	21	3457.9550	14	3374.1641	-7
31.0	-	-	3439.3623	10	3349.8868	-13
33.0	3517.5203	0	3419.5551	-11		
35.0	3502.1390	1	3398.5422	24		
37.0			3376.3128	-2		

B. 1-0 BAND

J	R_{ff}	O-C	Q_{ef}	O-C	P_{ff}	O-C
2.0	4982.8587	-4	4974.2295	2		
4.0	4986.2337	5	4971.8525	4	4960.3433	-29
6.0	4988.2456	-2	4968.1160	-6	4950.8623	13
8.0	4988.8964	0	4963.0236	4	4940.0202	-10
10.0	4988.1832	-2	4956.5723	4	4927.8291	4
12.0	4986.1057	-7	4948.7628	-2	4914.2840	-6
14.0	4982.6653	7	4939.5966	-7	4899.3925	15
16.0	4977.8571	2	4929.0741	-8	4883.1490	-2
18.0	4971.6830	0	4917.1957	-9	4865.5630	17
20.0	4964.1426	6	4903.9630	0	4846.6270	-18
22.0	4955.2342	5	4889.3721	-25	4826.3531	-8
24.0	4944.9563	-10	4873.4318	-5	4804.7440	54
26.0	-	-	4856.1368	-2	4781.7982	135
28.0	-	-	4837.4906	11	4757.4861	-83
30.0	4905.9165	-11	4817.4888	-20	4731.8729	27
32.0	4890.1697	30	4796.1428	7		
34.0			4773.4450	7		
36.0			-	-		

J	R_{ee}	O-C	Q_{fe}	O-C	P_{ee}	O-C
1.0	4980.6624	0				
3.0	4984.7193	7	4973.2110	-18		
5.0	4987.4155	-1	4970.1599	0	4955.7797	8
7.0	4988.7544	20	4965.7512	6	4945.6232	19
9.0	4988.7301	21	4959.9906	58	4934.1149	33
11.0	4987.3420	7	4952.8626	-2	4921.2519	6
13.0	4984.5922	5	4944.3848	-4	4907.0388	-30
15.0	4980.4797	15	4934.5518	-5	4891.4832	-19
17.0	4975.0004	2	4923.3647	0	4874.5811	-17
19.0	4968.1578	8	4910.8222	-6	4856.3371	4
21.0	4959.9473	-8	4896.9271	-3	4836.7461	-23
23.0	4950.3772	42	4881.6801	9	4815.8216	14
25.0	4939.4304	-7	4865.0785	-3	4793.5523	-15
27.0	-	-	4847.1294	21	4769.9512	-3
29.0	4913.4469	7	4827.8253	-1	4745.0164	10
31.0	4898.4024	0	4807.1746	2		
33.0			4785.1741	0		
35.0			4761.8283	-1		
37.0			4737.1351	-9		

C. 3-1 BAND

J	R_{ff}	O-C	Q_{ef}	O-C	P_{ff}	O-C
2.0	6099.0536	13	6090.6223	-28		
4.0	6102.0552	-15	6088.0121	-14	-	-
6.0	6103.5729	69	6083.9098	0	6067.0568	-27
8.0	6103.5726	-62	6078.3134	-4	6055.8547	20
10.0	6102.0947	2	6071.2262	0	6043.1577	11
12.0	6099.1113	-5	6062.6462	-9	6028.9790	-7
14.0	6094.6309	7	6052.5776	7	6013.3136	-32
16.0	6088.6495	8	6041.0187	27	5996.1709	-8
18.0	6081.1684	17	6027.9647	-2	5977.5249	-214
20.0	6072.1796	-37	6013.4235	-7	5957.4418	-5
22.0	6061.7003	19	5997.3952	5	5935.8640	23
24.0	-	-	5979.8772	4	5912.8084	23
26.0	-	-	5960.8679	-34		
28.0	-	-	-	-		
30.0	-	-	5918.4027	12		

	R_{ee}	O-C	Q_{fe}	O-C	P_{ee}	O-C
1.0	6096.9933	32				
3.0	6100.7462	25	6089.5081	-	6081.0760	-50
5.0	6103.0021	-20	6086.1526	-13	6072.1124	17
7.0	6103.7701	-1	6081.3091	-	6061.6512	-16
9.0	6103.0428	16	6074.9741	2	6049.7095	6
11.0	6100.8151	-8	6067.1482	-3	6036.2802	-1
13.0	6097.0933	-2	6057.8337	2	6021.3679	-8
15.0	6091.8738	6	6047.0309	19	6004.9763	6
17.0	6085.1548	5	6034.7426	69	5987.1028	-1
19.0	6076.9356	-3	6020.9540	-	5967.7539	16
21.0	6067.2138	-38	6005.6818	-27	5946.9247	-7
23.0	6056.0037	49	5988.9280	-	5924.6233	-11
25.0	-	-	5970.6847	-4	5900.8517	6
27.0	-	-	5950.9560	-7		
29.0	-	-	5929.7439	2		

D. 5-2 BAND

J	R_{ff}	O-C	Q_{ef}	O-C	P_{ff}	O-C
2.0	7148.4881	0				
4.0	7151.1220	0	7137.4207	29		
6.0	7152.1258	-6	7132.9446	-2	7116.5012	-2
8.0	7151.5018	14	7126.8480	23	7104.9288	18
10.0	7149.2427	0	7119.1200	-5	7091.7288	-24
12.0	7145.3493	-34	7109.7659	-38	7076.9097	-64
14.0	7139.8329	32	7098.7956	18	-	-

Note. Observed minus calculated line positions are in units of 10^{-4} cm^{-1}.

[a] Perturbed.

TABLE I—*Continued*

D. 5-2 BAND

J	R_{ff}	O-C	Q_{ef}	O-C	P_{ff}	O-C
16 0	7132.6710	-15	7086.1907	-22	-	-
18 0	7123.8802	-6	7071.9676	-4	7022.7601	-103
20.0	7113.4539	0	7056.1209	14	7001.4981	37
22.0	7101.3897	-14	7038.6460	-20		
24.0	7087.6907	-15				

J	R_{ee}	O-C	Q_{fe}	O-C	P_{ee}	O-C
1.0	7146.5615	7				
3.0	-	-				
5.0	7151.8337	1	7135.3886	-16	7121.6841	-19
7.0	7152.0291	13	7130.1094	3	7110.9283	8
9.0	7150.5335	10	7123.1947	-85	7098.5474	-11
11.0	-	-	7114.6743	11	7084.5409	-99
13.0	7142.8313	16	-	-	-	-
15.0	7136.5009	3	7092.7415	0	7051.7078	21
17.0	7128.5359	-27	-	-	-	-
19.0	7118.9691	258*	7064.3403	221*	-	-
21.0	-	-	-	-		
23.0	-	-	7029.4157	78		

E. 0-1 BAND

J	R_{ff}	O-C	Q_{ef}	O-C	P_{ff}	O-C
2 0	2014.5833	53	2005.8403	-67		
4.0	-	-	-	-	1992.3003	-34
6.0	2021.3208	12	2000.9545	1	-	-
8.0	-	-	1996.8811	34	1973.6067	4
10.0	2023.6876	-90	1991.7142	0	1962.6367	25
12.0	2023.2441	-21	1985.4621	-26	1950.5759	-59
16.0	2015.3280	-25	1969.7089	0	1930.5293	11
18.0	2010.5036	16	1960.2021	-16		
20.0	2004.5685	-89	1949.6151	2		
22.0	2001.3114	9	1937.9472	44		
24.0	1997.5551	-16	1925.1880	-5		
26.0	1993.7575	-30				

J	R_{ee}	O-C	Q_{fe}	O-C	P_{ee}	O-C
3.0	-	-	2005.0342	3	1996.2942	-87
5.0	2020.0488	0	-	-	-	-
7.0	-	-	-	-	1978.6907	-68
9.0	2023.5334	41	1994.4499	8	1968.2725	-1
11.0	2023.6327	-7	1988.7479	-27	1956.7687	3
13.0	2021.7071	49	1981.9687	9	-	-
15.0	2017.3947	16	1974.1023	13	1937.4568	56
17.0	2013.1244	-20	1965.1452	-56	1915.7976	17
19.0	-					
21.0	-					
23.0	-					
25.0	1993.7575	-30				

F. 2-1 BAND

J	R_{ff}	O-C	Q_{ef}	O-C	P_{ff}	O-C
2.0	4760.3878	10	4751.8604	22	4742.3051	-89
4.0	-	-	4749.4834	0	4733.5856	51
6.0	4765.6434	-11	4745.7511	-4	4723.4985	38
8.0	4766.2312	-12	4740.6625	-5	4712.0565	-15
10.0	4765.4635	51	4734.2167	-13	4699.2715	-6
12.0	4763.3223	9	4726.4168	-1	4685.1372	-13
14.0	4759.8210	2	4717.2598	-2	4669.6691	102
16.0	4754.9620	63	4706.7475	-3	4652.8357	8
18.0	4748.7250	-4	4694.8807	-2	4634.6722	39
20.0	4741.1288	-7	4681.6604	5	4615.1598	-12
22 0	4732.1673	0	4667.0872	19	4594.3160	10
24.0	4721.8479	97	4651.1588	8	4572.1342	20
26.0	4710.1430	10	4633.8796	9	4548.6146	0
28.0	4697.0772	-9	4615.2508	25		
30.0	4682.6445	-19	4595.2685	6		
32.0			4573.9338	-44		

J	R_{ee}	O-C	Q_{fe}	O-C	P_{ee}	O-C
1.0	4758.2202	-29				
3.0	4762.2134	0	4750.8375	-51	4738.1154	28
5.0	4764.8500	40	4747.7934	6	4728.7014	29
7.0	4766.1192	-2	4743.3882	5	4717.9291	-21
9.0	4766.0326	-4	4737.6261	-13	4705.8127	2
11.0	4764.5903	46	4730.5128	4	4692.3440	3

F. 2-1 BAND

J	R_{ff}	O-C	Q_{ef}	O-C	P_{ff}	O-C
13.0	4761.7784	17	4722.0429	0	4677.5229	-34
15.0	4757.6051	0	4712.2188	-7	4661.3618	-5
17.0	4752.0706	4	4701.0425	-1	4643.8487	-46
19.0	4745.1706	-8	4688.5138	9	4625.0035	23
21.0	4736.9074	-7	4674.6291	-15	4604.8063	-14
23.0	4727.2783	-16	4659.3985	15	4583.2798	48
25.0	4716.2831	-30	-	-	4560.4050	0
27.0	4703.9253	-13	4624.8738	-41		
29.0	4690.2103	94	4605.5939	-4		
31.0	4675.1096	8	4584.9651	23		

G. BAND 4-2

J	R_{ff}	O-C	Q_{ef}	O-C	P_{ff}	O-C
2.0	5855.2433	-29	5846.9292	85		
4.0	5858.1817	-41	5844.3126	7		
6.0	5859.6359	40	5840.2140	14		
8.0	5859.5813	-17	5834.6240	12		
10.0	5858.0346	-39	5827.5433	5	5799.8115	-24
12.0	5854.9949	-25	5818.9665	-64	5785.7210	90
14.0	5850.4670	81	5808.9148	11	5770.1300	22
16.0	5844.4270	50	5797.3666	12	5753.0616	-15
18.0	5836.8849	-12	5784.3255	-29	5734.5176	-22
20.0	5827.8506	0	5769.8014	-21	5714.49[illegible]3	-3
22.0	5817.3188	39	5753.7901	-12		
24.0	5805.2822	38	5736.2905	-20		
26.0			5717.3095	16		
28.0			5696.8405	23		
30.0			5674.8891	48		

J	R_{ee}	O-C	Q_{fe}	O-C	P_{ee}	O-C
1.0	5853.2165	-5				
3.0	5856.9146	96	5845.8096	47		
5.0	5859.1054	41	5842.4523	-18		
7.0	5859.8097	48	5837.6125	-19		
9.0	5859.0138	-9	5831.2855	-4	5806.3254	-2
11.0	5856.7317	17	5823.4719	29	5792.9763	31
13.0	5852.9471	25	5814.1678	40	5778.1382	-10
15.0	5847.6733	4	5803.3697	-10	5761.8273	17
17.0	5840.9054	63	5791.0831	-73	5744.02[illegible]7	-81
19.0	5832.6503	229*	5777.3397	162*	5724.7886	228*
21.0	5822.8808	235*	5762.0893	190*		
23.0	5811.5938	56	5745.3290	-26		
25.0	5798.8227	32	5727.1216	134		
27.0			5707.3956	-52		
29.0			5686.2076	-27		
31.0			5663.5341	-35		

H. 3-2 BAND

J	R_{ff}	O-C	Q_{ef}	O-C	P_{ff}	O-C
2.0	4539.3164	-97				
4.0	4542.5663	40	-	-	4517.2900	-16
6.0	4544.4484	-79	4524.8001	0	4507.9476	-22
8.0	4544.9878	47	4519.7129	-51	4497.2550	-18
10.0	4544.1514	18	4513.2777	-36	4485.2060	-80
12.0	4541.9514	-37	4505.4829	-74	4471.8157	-72
14.0	4538.4058	69	4496.3456	0	4457.0866	11
16.0	4533.4778	-22	4485.8476	2	4440.9966	-65
18.0	-	-	4473.9944	-21	4423.5794	14
20.0	4519.5500	-27	4460.7967	30	4404.8167	49
22.0	4510.5461	28	4446.2360	-36	4384.7124	58
24.0	4500.1714	21	4430.3319	-32		
26.0			4413.0867	55		
28.0			4394.4702	-86		

J	R_{ee}	O-C	Q_{fe}	O-C	P_{ee}	O-C
3.0	4541.1130	-72	4529.8828	-19		
5.0	4543.6865	-23	4526.8532	145	-	-
7.0	4544.8988	-13	4522.4434	44	4502.7745	-82
9.0	4544.7542	8	4516.6878	18	4491.4194	-15
11.0	4543.2482	8	4509.5794	-5	4478.7137	19
13.0	4540.3834	19	4501.1239	25	4464.6594	27
15.0	-	-	4491.3108	0	4449.2510	-64
17.0	4530.5649	-22	4480.1479	-7	4432.5060	-99
19.0	4523.6463	288*	4467.6561	205*	4414.4626	287*
21.0	-	-	4453.7938	213*	4395.0410	276*
23.0	4505.6376	68	4438.5556	-43		
25.0	4494.5965	36	-	-		
27.0			4404.0889	-18		
29.0			4384.8315	-44		

TABLE II

Observed Line Positions of the $B'\,^1\Sigma_g^+ - A\,^1\Pi_u$ Transition of C_2 (in cm^{-1})

A. 0-0 BAND

J	R_{ee}	O-C	P_{ee}	O-C	J	Q_{ef}	O-C
1.0	6933.7527	-48	6924.9053	-6			
3.0	6938.3299	-1	6917.6761	-20	2.0	6927.3239	-5
5.0	6941.8384	4	6909.3888	-15	4.0	6925.4629	-6
7.0	6944.2805	6	6900.0463	27	6.0	6922.5386	-3
9.0	6945.6536	-5	6889.6398	8	8.0	6918.5507	1
11.0	6945.9601	7	6878.1776	1	10.0	6913.4979	1
13.0	6945.1939	-1	6865.6618	18	12.0	6907.3814	2
15.0	6943.3574	7	6852.0873	-2	14.0	6900.1991	-6
17.0	6940.4449	-12	6837.4613	0	16.0	6891.9533	-2
19.0	6936.4610	-5	6821.7816	-10	18.0	6882.6419	-7
21.0	6931.4011	-9	6805.0528	-1	20.0	6872.2624	-50
23.0	6925.2655	-21	6787.2731	-9	22.0	6860.8281	-4
25.0	6918.0597	10	6768.4476	-8	24.0	6848.3269	0
27.0			6748.5861	71	26.0	6834.7649	4
29.0			6727.6719	28	28.0	6820.1421	-11
					30.0	6804.4626	-38

B. 0-1 BAND

J	R_{ee}	O-C	P_{ee}	O-C	J	Q_{ef}	O-C
1.0			5340.8905	-36			
3.0	5354.4885	-1	5333.8347	-20	2.0	5343.3805	3
5.0	5358.3045	12	5325.8562	5	4.0	5341.7580	-4
7.0	5361.1876	-6	5316.9542	22	6.0	5339.2097	8
9.0	5363.1437	17	5307.1275	7	8.0	5335.7322	4
11.0	5364.1631	1	5296.3818	7	10.0	5331.3291	21
13.0	5364.2515	17	5284.7175	17	12.0	5325.9949	7
15.0	5363.4009	-2	5272.1321	1	14.0	5319.7336	4
17.0	5361.6154	-2	5258.6305	-3	16.0	5312.5438	-1
19.0	5358.8915	-11	5244.2132	-5	18.0	5304.4262	-2
21.0	5355.2292	-21	5228.8811	-11	20.0	5295.3797	-13
23.0	5350.6314	-3	5212.6378	-3	22.0	5285.4087	2
25.0	5345.0974	32	5195.4838	-1	24.0	5274.5115	17
27.0			5177.4238	11	26.0	5262.6878	12
29.0			5158.4593	16	28.0	5249.9430	16
31.0			5138.5942	6	30.0	5236.2766	-6
					32.0	5221.6982	-1

C. 1-0 BAND

J	R_{ee}	O-C	P_{ee}	O-C	J	Q_{ef}	O-C
1.0			8345.3900	-5			
3.0	8358.6052	3	8338.1018	20	2.0	8347.7422	-39
5.0	8361.8687	-135	8329.6626	-25	4.0	8345.7388	4
7.0	8364.0124	24	8320.0890	11	6.0	8342.5837	4
9.0	8364.9889	21	8309.3715	23	8.0	8338.2798	-9
11.0	8364.8124	9	8297.5067	34	10.0	8332.8305	-2
13.0	8363.4843	15	8284.5100	-20	12.0	8326.2341	8
15.0	8361.0029	30	8270.3756	-7	14.0	8318.4894	8
17.0	8357.3584	-34	8255.0939	-106	16.0	8309.5968	0
19.0	8352.5630	-53	8238.7011	27	18.0	8299.5585	1
21.0	8346.6156	-36	8221.1576	-21	20.0	8288.3758	14
23.0	8339.5139	-11	8202.4987	74	22.0	8276.0487	29
25.0	8331.2579	12	8182.6925	-33	24.0	8262.5752	8
27.0	8321.8454	-5	8161.7886	115	26.0	8247.9689	64
29.0	8311.2879	24	8139.7393	3	28.0	8232.2146	14

D. 1-2 BAND

J	R_{ee}	O-C	P_{ee}	O-C	J	Q_{ef}	O-C
1.0			5201.5842	1			
3.0	5215.1378	-22	5194.6344	-5	2.0	5204.0762	-1
5.0	5219.0327	4	5186.8152	0	4.0	5202.5464	-5
7.0	5222.0487	4	5178.1258	-3	6.0	5200.1432	-3
9.0	5224.1884	16	5168.5689	-1	8.0	5196.8672	10
11.0	5225.4466	0	5158.1461	9	10.0	5192.7142	-5
13.0	5225.8244	-21	5146.8560	1	12.0	5187.6843	-52
15.0			5134.7035	9	14.0	5181.7917	10
17.0	5223.9428	-15	5121.6848	-21	16.0	5175.0188	3
19.0	5221.6973	162[a]	5107.8338	227[a]	18.0	5167.3736	-1
21.0	5218.5575	210[a]	5093.0969	199[a]	20.0	5158.8567	-5
23.0	5214.5109	-1	5077.4872	0	22.0	5149.4703	-2
25.0	5209.6062	1	5061.0457	4	24.0	5139.2175	20
27.0	5203.8204	-31	5043.7539	-7	26.0	5128.0960	15
29.0			5025.6179	-19	28.0	5116.1087	-20

E. 2-1 BAND

J	R_{ee}	O-C	P_{ee}	O-C	J	Q_{ef}	O-C
1.0	8189.6339	4					
3.0	8194.1073	-5	8173.7266	21	4.0	8181.3747	-30
5.0	8197.5020	13	8165.4765	16	6.0	8178.4043	-19
7.0	8199.7992	-112	8156.1504	10	8.0	8174.3543	2
9.0	8201.0334	-24	8145.7491	0	10.0	8169.2215	6
11.0	8201.1755	0	8134.2740	-9	12.0	8163.0078	11
13.0	8200.2275	-5	8121.7293	10	14.0	8155.7123	8
15.0	-	-	8108.1096	-6	16.0	8147.3365	9
17.0	8195.0692	3	8093.4215	-10	18.0	8137.8797	1
19.0	8190.8570	8	8077.6668	-1	20.0	8127.3420	-25
21.0	8185.5564	13	8060.8461	3	22.0	8115.7322	1
23.0	8179.1682	15	-	-	24.0	8103.0482	35
25.0	8171.6923	-6	8024.0238	49	26.0	8089.2835	-19
27.0	8163.1403	30	8004.0192	-22	28.0	8074.4536	-53

F. 3-2 BAND

J	R_{ee}	O-C	P_{ee}	O-C	J	Q_{ef}	O-C
1.0	8050.8544	-16	8042.1679	-1			
3.0	8055.3840	-7	8035.1165	-6	2.0	8044.5578	-7
5.0	8058.9090	56	8027.0613	15	4.0	8042.7872	-44
7.0	8061.4099	2	8017.9971	-2	6.0	8040.0107	-40
9.0	8062.9014	-2	8007.9307	3	8.0	8036.2285	10
11.0	8063.3752	-23	7996.8597	-3	10.0	8031.4295	-2
13.0	8062.8351	-3	7984.7900	32	12.0	8025.6169	36
15.0	8061.2732	0	7971.7108	-6	14.0	8018.8015	20
17.0	8058.6891	3	7957.6334	-7	16.0	8010.9678	22
19.0	8055.1105	307[a]	7942.5819	264[a]			

Note. Observed minus calculated line positions are in units of 10^{-4} cm^{-1}.

[a] Perturbed.

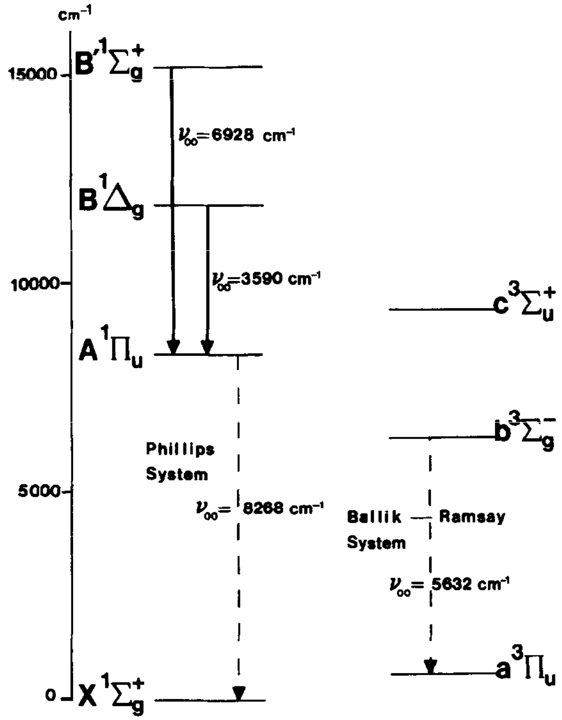

FIG. 1. Energy level diagram of the low-lying states of C_2.

Very recently, a new $1\,^1\Delta_u$ state was discovered by Goodwin and Cool (7). Two-photon fragmentation of acetylene followed by resonance-enhanced multiphoton ionization of C_2 located the $1\,^1\Delta_u$ state 57 719 cm^{-1} above the $X\,^1\Sigma_g^+$ state.

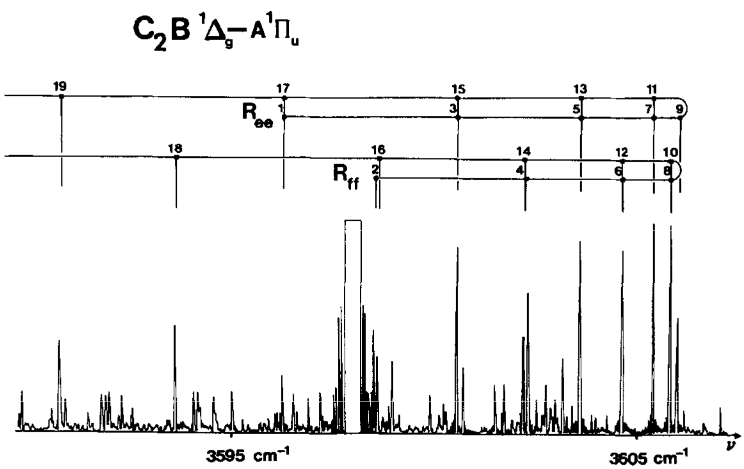

FIG. 2. A portion of the 0–0 band of the $B^1\Delta_g$–$A^1\Pi_u$ transition of C_2 near the R bandhead.

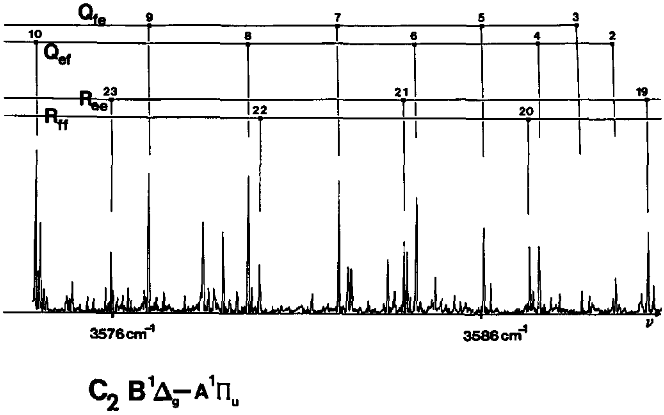

FIG. 3. A portion of the 0–0 band of the $B^1\Delta_g$–$A^1\Pi_u$ transition of C_2 near the band origin.

II. EXPERIMENT

The experimental procedures are described in the previous paper (*2*).

III. RESULTS AND DISCUSSION

Our method of analysis is described in the paper on the Phillips system (*2*). The spectra were very congested, so the analysis proceeded by bootstrap calculation. First, a crude estimate of the location of a band was made and some *Q*-branch lines were picked out and assigned. A preliminary fit predicted the remaining lines in the band which were then measured and included in the fit. The search for new bands was guided by a preliminary calculation of Franck–Condon factors.

Ultimately, eight bands of the $B^1\Delta_g$–$A^1\Pi_u$ transition were analyzed, 0–0, 1–0, 3–1, 5–2, 0–1, 2–1, 4–2, and 3–2, while six bands were found for the $B'\,^1\Sigma_g^+$–$A^1\Pi_u$ transition, 0–0, 0–1, 1–0, 1–2, 2–1, and 3–2. The line positions of the $B^1\Delta_g$–$A^1\Pi_u$ and $B'\,^1\Sigma_g^+$–$X^1\Pi_u$ bands are reported in Tables I and II, respectively. An energy level diagram and sample spectra are provided in Figs. 1–4.

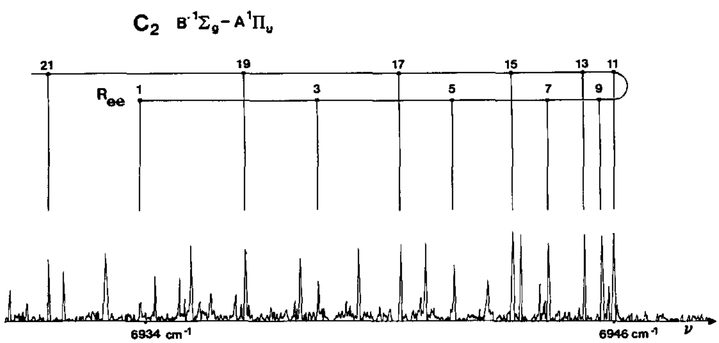

FIG. 4. A portion of the 0–0 band of the $B'\,^1\Sigma_g^+$–$A^1\Pi_u$ transition of C_2 near the *R* bandhead.

TABLE III

Molecular Constants for the $B^1\Delta_g$ state of C_2 (in cm^{-1})

Constant	v = 0	v = 1	v = 2	v = 3	v = 4	v = 5
T_v	11859.0980(2)[a]	13243.6377(3)	14605.3115(4)	15944.1799(4)	17260.3030(12)	18553.7486(9)
B_v	1.4552733(21)	1.4384277(24)	1.4215521(28)	1.4046420(30)	1.3877210(80)	1.3707393(81)
$10^6 \times D_v$	6.32590(125)	6.34196(162)	6.3575(24)	6.3671(29)	6.4035(85)	6.3883(137)

[a] The numbers in parentheses are one standard deviation in the last digit.

The line positions of Tables I and II, as well as all of our observed line positions of the Phillips system (Table I of the preceding paper), were fitted simultaneously using the customary rotational energy level expression (*2*). The spectroscopic constants of the $B^1\Delta_g$ and $B'\,^1\Sigma_g^+$ states from this global fit are reported in Tables III and IV, respectively.

The constants of the $B^1\Delta_g$ state are very well behaved, but those of the $B'\,^1\Sigma_g^+$ state showed some evidence of interaction with other states. For example, $v = 0$, 1, and 2 of the $B'\,^1\Sigma_g^+$ state required H's, although none of the vibrational levels of the $B^1\Delta_g$ state required any. The only local perturbations present in the $B'\,^1\Sigma_g^+$–$A^1\Pi_u$ or the $B^1\Delta_g$–$A^1\Pi_u$ transitions are for $v = 2$, $J = 19e$, $21e$ of the lower $A^1\Pi_u$ state (*2*).

The constants of Tables III and IV were converted to equilibrium molecular constants (Table V) with the expressions listed in the previous paper (*2*). The global interaction of the $B'\,^1\Sigma_g^+$ state with other states (particularly the $X^1\Sigma_g^+$ state) is also reflected in the equilibrium molecular constants (Table V). The $\omega_e x_e$ value is very small (2.57 cm^{-1}) compared to the expected value of 7.65 cm^{-1} computed from α_e with the Pekeris relationship (*8*). The $G(v)$ and B_v expansions require as many parameters as data points to reproduce the data points within the experimental error in the $B'\,^1\Sigma_g^+$ state.

The $X^1\Sigma_g^+$ and $B'\,^1\Sigma_g^+$ states have the same symmetry, but nominally come from different configurations (π^4 for $X^1\Sigma_g^+$ and $\pi^2\sigma^2$ for $B'\,^1\Sigma_g^+$). In the ground $X^1\Sigma_g^+$

TABLE IV

Molecular Constants for the $B'\,^1\Sigma_g^+$ State of C_2 (in cm^{-1})

Constant	v = 0	v = 1	v = 2	v = 3
T_v	15196.5116(4)[a]	16616.9962(4)	18036.5144(8)	19457.8501(9)
B_v	1.4753124(42)	1.4648230(52)	1.4561354(112)	1.4478630(171)
$10^6 \times D_v$	6.7810(95)	6.6208(137)	6.744(35)	6.881(63)
$10^{10} \times H_v$	2.220(66)	2.167(107)	3.38(30)	-

[a] The numbers in parentheses are one standard deviation in the last digit.

TABLE V

Equilibrium Molecular Constants for the $B^1\Delta_g$ and $B'\,^1\Sigma_g^+$ States of C_2 (in cm^{-1})

State	ω_e	$\omega_e x_e$	$\omega_e y_e$
$B^1\Delta_g$	1407.46529(134)[a]	11.47937(60)	0.010256(73)
$B'\,^1\Sigma_g^+$	1424.11890[b]	2.57113[b]	0.46398[b]
	B_e	α_e	$\gamma_e \times 10^5$
$B^1\Delta_g$	1.4636853(34)	0.0168161(35)	-1.503(72)
$B'\,^1\Sigma^+$	1.481006(296)	0.011752(459)	67.18(1387)
	$D_e \times 10^6$	$\beta_e \times 10^7$	
$B^1\Delta_g$	6.3188(19)	0.1492(113)	
$B'\,^1\Sigma_g^+$	6.8596(136)	-1.581(143)	
	r_e	T_e	
$B^1\Delta_g$	1.385475 Å	12082.3360(40)	
$B'\,^1\Sigma_g^+$	1.377350 Å	15409.1390(39)	

[a] The numbers in parentheses are one standard deviation.

[b] An exact fit.

TABLE VI

RKR Turning Points of the $B^1\Delta_g$ State of C_2

v	E_v (cm^{-1})[a]	R_{min} (Å)	R_{max} (Å)
0.0	700.9482[a]	1.32618	1.45299
0.5	1396.0803	1.30375	1.48370
1.0	2085.4881	1.28732	1.50847
1.5	2769.1793	1.27398	1.53023
2.0	3447.1616	1.26260	1.55009
2.5	4119.4426	1.25259	1.56864
3.0	4786.0301	1.24363	1.58621
3.5	5446.9318	1.23549	1.60303
4.0	6102.1553	1.22802	1.61925
4.5	6751.7084	1.22111	1.63498
5.0	7395.5987	1.21467	1.65032

[a] Relative to the bottom of the $B^1\Delta_g$ well. To convert the origin of the E_v scale to the bottom of the $X^1\Sigma_g^+$ well, 12082.1338 cm^{-1}, must be added. This number was calculated using the experimental value of 11859.0980 cm^{-1} for T_{00}. Note that the E_v values in this table include the Dunham Y_{00} correction for the $B^1\Delta_g$ state.

TABLE VII

RKR Turning Points for the $B'\,^1\Sigma_g^+$ State of C_2

v	E_v (cm^{-1})[a]	R_{min} (Å)	R_{max} (Å)
0.0	712.7427	1.31765	1.44348
0.5	1423.2797	1.29473	1.47268
1.0	2133.2272	1.27777	1.49575
1.5	2842.9331	1.26387	1.51558
2.0	3552.7454	1.25191	1.53331
2.5	4263.0120	1.24132	1.54950
3.0	4974.0809	1.23176	1.56448

[a] Relative to the bottom of the $B'^1\Sigma_g^+$ well. To convert the origin of the E_v scale to the bottom of the $X^1\Sigma_g^+$ well, 15407.7529 cm^{-1} must be added. This number was calculated using the experimental T_{00} value of 15196.5116 cm^{-1}. Note that the E_v values in this table include the Dunham Y_{00} correction for the $B'^1\Sigma_g^+$ state.

state, the $G(v)$ and B_v polynomial expansions are also not very satisfactory representations of the vibrational and rotational energy levels. The interaction between $X\,^1\Sigma_g^+$ and $B'\,^1\Sigma_g^+$ will change as a function of r and may cause the $B'\,^1\Sigma_g^+$ and $X\,^1\Sigma_g^+$ potential energy curves to have peculiar shapes.

The RKR potential energy curves (Tables VI and VII) were calculated from the equilibrium molecular constants (Table V). The RKR points for the $B'\,^1\Sigma_g^+$, $B\,^1\Delta_g$, $A\,^1\Pi_u$, and $X\,^1\Sigma_g^+$ states are plotted in Fig. 1 of the previous paper.

The RKR potential points were used to calculate the $B\,^1\Delta_g$–$A\,^1\Pi_u$ (Table VIII) and $B'\,^1\Sigma_g^+$–$A\,^1\Pi_u$ (Table IX) Franck–Condon factors. We found all of the bands expected on the basis of Franck–Condon factors, confirming our vibrational assignment.

TABLE VIII

Franck–Condon Factors for the $B\,^1\Delta_g$–$A\,^1\Pi_u$ Transition of C_2

v' \ v"	0	1	2	3	4	5
0	0.544 E0	0.354 E0	0.898 E-1	0.113 E-1	0.754 E-3	0.253 E-4
1	0.306 E0	0.825 E-1	0.378 E0	0.193 E0	0.371 E-1	0.332 E-2
2	0.108 E0	0.263 E0	0.796 E-3	0.273 E0	0.270 E0	0.753 E-1
3	0.314 E-1	0.181 E0	0.138 E0	0.543 E-1	0.148 E0	0.307 E0
4	0.825 E-2	0.789 E-1	0.187 E0	0.409 E-1	0.122 E0	0.553 E-1
5	0.206 E-2	0.278 E-1	0.119 E0	0.146 E0	0.168 E-2	0.156 E0

TABLE IX

Franck–Condon Factors for the $B'\,{}^1\Sigma_g^+$–$A\,{}^1\Pi_u$ Transition of C_2

v' \ v"	0	1	2	3	4	5
0	0.635 E0	0.305 E0	0.556 E-1	0.438 E-2	0.106 E-3	0.147 E-6
1	0.275 E0	0.199 E0	0.389 E0	0.123 E0	0.126 E-1	0.276 E-3
2	0.723 E-1	0.306 E0	0.389 E-1	0.378 E0	0.182 E0	0.220 E-1
3	0.144 E-1	0.140 E0	0.250 E0	0.688 E-3	0.338 E0	0.228 E0

The observed spectroscopic constants for the $B\,{}^1\Delta_g$ and $B'\,{}^1\Sigma_g^+$ states are in agreement with the excellent recent theoretical calculations (Table X). For example, the error in the T_e values is less than 1000 cm^{-1} and r_e is predicted to within 0.03 Å.

IV. CONCLUSION

We have observed two new infrared electronic transitions of C_2, $B\,{}^1\Delta_g$–$A\,{}^1\Pi_u$ and $B'\,{}^1\Sigma_g^+$–$A\,{}^1\Pi_u$, by Fourier transform emission spectroscopy of hydrocarbon discharges. These transitions involve low-lying states so they should be observable in comets, stellar atmospheres, and flames.

TABLE X

Comparison of Experimental Spectroscopic Constants of the $B\,{}^1\Delta_g$ and $B'\,{}^1\Sigma_g^+$ States of C_2 with ab Initio Predictions

State		T_e (cm^{-1})	ω_e (cm^{-1})	$\omega_e x_e$ (cm^{-1})	r_e (Å)	α_e (cm^{-1})
$B^1\Delta_g$	(expt.)	12082	1407	11	1.385	0.017
	(theory)[a]	11670	1350	13	1.408	-
	(theory)[b]	12800	1322	14	1.41	0.017
$B'^1\Sigma_g^+$	(expt.)	15409	1424	3	1.377	0.012
	(theory)[a]	14670	1368	8	1.402	-
	(theory)[b]	14600	1322	20	1.41	0.019

[a] Reference 6.

[b] Reference 5.

ACKNOWLEDGMENTS

The National Solar Observatory is operated by the Association of Universities for Research in Astronomy, Inc., under contract with the National Science Foundation. We thank J. Wagner, R. Ram, and G. Ladd for assistance in acquiring our C_2 spectra. Acknowledgment is made to the donors of the Petroleum Research Fund, administered by the American Chemical Society, for partial support of this work. Some support was also provided by the Air Force Astronautics Laboratory, Grant No. F-04611-11187-K-0020. We thank J. Black for a copy of Ref. (*6*) and for discussions on the spectroscopic observations of C_2 in space.

RECEIVED: May 16, 1988

REFERENCES

1. P. F. BERNATH, S. A. ROGERS, L. C. O'BRIEN, C. R. BRAZIER, AND A. D. MCLEAN, *Phys. Rev. Lett.* **60**, 197–199 (1988).
2. M. DOUAY, R. NIETMANN, AND P. F. BERNATH, *J. Mol. Spectrosc.* **131**, 250–260 (1988).
3. P. F. FONGERE AND R. K. NESBET, *J. Chem. Phys.* **44**, 285–298 (1966).
4. J. BARSUHN, *Z. Naturforsch., A* **27**, 1031–1041 (1972).
5. K. KIRBY AND B. LIU, *J. Chem. Phys.* **70**, 893–900 (1979).
6. R. KLOTZ AND S. D. PEYERIMHOFF, private communication via J. Black and E. van Dishoeck.
7. P. M. GOODWIN AND T. A. COOL, *J. Chem. Phys.* **88**, 4548–4549 (1988).
8. G. HERZBERG, "Spectra of Diatomic Molecules," 2nd ed., p. 108, Van Nostrand–Reinhold, New York, 1950.